Hindawi Publishing Corporation
Journal of Nanomaterials
Volume 2012, Article ID 154278, 8 pages
doi:10.1155/2012/154278

Research Article

Absorption Properties of Hybrid Composites of Gold Nanorods and Functionalized Single-Walled Carbon Nanotubes

Deok-Jin Yu,[1] D. Ganta,[1] Elijah Dale,[1] A. T. Rosenberger,[1] James P. Wicksted,[1] and A. Kaan Kalkan[2]

[1] *Department of Physics, Oklahoma State University, Stillwater, OK 74078, USA*
[2] *Department of Mechanical and Aerospace Engineering, Oklahoma State University, Stillwater, OK 74078, USA*

Correspondence should be addressed to Deok-Jin Yu, deokjin.yu@okstate.edu and James P. Wicksted, james.wicksted@okstate.edu

Received 10 October 2011; Accepted 15 December 2011

Academic Editor: Kin Tak Lau

We report on the optical properties of fabricated nanohybrid structures containing Au nanorods and functionalized single-walled carbon nanotubes in aqueous solutions. In particular, the absorption spectra of these hybrid materials are studied as a function of the concentration of the functionalized single-walled carbon nanotubes as well as the evolution time following preparation. The absorption spectra show a red shift of the longitudinal plasmon mode of the Au nanorods along with the emergence of broadened structures at wavelengths between 1000 and 1100 nm. These results, supported by TEM images, indicate the self-assembly of the Au nanorods forming on the sidewalls of the functionalized SWNTs driven by polyelectrolyte interactions.

1. Introduction

Nanostructures have generated potential interest as building blocks for electronic/photonic devices, nanocomposites, and chemical/biological sensors [1–6]. However, there are still limitations in controlling the shapes, orientations, and assembly of nanoscale. Recently, aligned hybrid nanostructures have been achieved which consist of metallic nanoparticles or nanorods and single-walled carbon nanotubes (SWNTs) [7, 8]. In particular, electromagnetically coupled gold nanoparticles provide unique and tunable optical properties resulting from their surface plasmon resonance effects [9–11]. Gold nanorods have both transverse and longitudinal plasmon modes which depend on their size, shape, and aspect ratio.

Here, we performed a systematic study of the optical properties and interactions of gold nanorods and functionalized single-walled carbon nanotubes (SWNT-PSS^{n-}) as the concentration of the latter is varied and the time following preparation of these mixed hybrid composites in aqueous solution is changed. Gold nanorods were prepared by a seed-mediated procedure pioneered by Gole and Murphy [12]. The excessive surfactant (hexadecyltrimethylammonium bromide, CTAB) was removed from the nanorod suspension by centrifugation, decant, and resuspension with 18.2 MΩ deionized water. The SWNTs were covalently grafted with an anion polyelectrolyte in order to provide water-soluble composites of nanotubes [13]. This technique is useful for compromising covalent bonding of the SWNTs which limits the applications of carbon nanotubes [14]. Using optical spectroscopy, we monitor the self-alignment of the Au nanorods on the functionalized SWNTs resulting in nanohybrid composites.

2. Experimental

Single-walled carbon nanotubes in the form of a 22 mg/g (aqueous gel type) were obtained from Southwest Nanotechnologies Inc., Norman, OK USA. Sodium 4-styrenesulfonate monomer (Mw ~70,000, powder), $HAuCl_4$-$3H_2O$ (99.9%), $NaBH_4$ (99%), ascorbic acid (99 + %), hexadecyltrimethylammonium bromide (CTAB (99%)), and $AgNO_3$ (99 + %) were purchased from Sigma-Aldrich. Ultrapure deionized water (18.2 MΩ·cm) was used for all solution preparations and experiments [15].

The preparation of the SWNT-PSS^{n-} composite was done by insitu polymerization. The synthesis of the functionalized SWNTs-PSS^{n-} was based on an established method

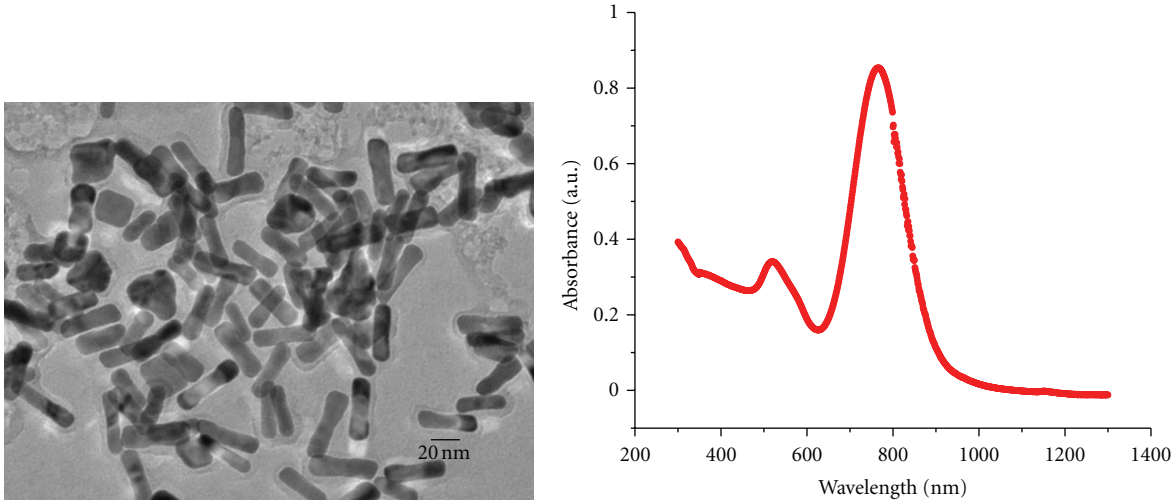

(a) (b)

Figure 1: (a) TEM image of gold nanorods synthesized by seed-mediated growth. (b) UV-Vis-IR spectrum of gold nanorods in DI water.

[16]. A 100 mL flask containing a mixture of 40 mg of pristine SWNT, 4.0 g of sodium 4-styrenesulfonate monomer, and 65 mL of deionized water was sonicated for 30 minutes followed by stirring for 4 hours. Then 40 mg of potassium peroxodisulfate ($K_2S_2O_8$) as a free radical initiator was added, and the mixture was degassed by a vacuum pump and refilled with nitrogen three times. The flask was sealed under vacuum: the synthesis was carried out in a 3 M thermostated oil at 65°C for 48 h. The reaction was then stopped by cooling to room temperature after which the flask was opened. The mixture was diluted to 500 mL with deionized water, then bath-sonicated for 1 hour. The supernatant was removed by gentle centrifugation, and extra free polymers were removed by ultracentrifugation (Eppendorf 5415 microcentrifuge). The resulting solution held 68 mg of SWNT-PSS^{n-} in 100 mL of water. This solution was then diluted so that the final prepared solution contained 0.02 g/L functionalized SWNTs.

In the preparation of Au nanorods, 0.250 mL of an aqueous 0.01 M solution of $HAuCl_4 \cdot 3H_2O$ was added to 7.5 mL of a 0.10 M CTAB solution in a glass tube. Then, 0.600 mL of an aqueous 0.01 M ice-cold $NaBH_4$ solution was quickly added and followed by rapid inversion mixing for 2 minutes. The solution developed a pale brown-yellow color and was maintained in a test tube at 25°C. This seed solution was used 2 hours after its preparation [17]. For making nanorods with aspect ratios of ~4.2, Murphy's method was used [17, 18]. 0.200 mL of an aqueous 0.01 M solution of $HAuCl_4 \cdot 3H_2O$ was added to 4.75 mL of a 0.10 M CTAB solution in a glass tube. Then 0.030 mL 0.01 M $AgNO_3$ solution was added. The solution was gently mixed. Then, 0.03 mL of 0.10 M ascorbic acid (AA) was added. The solution became colorless upon addition and mixing of AA. Finally, 0.010 mL of seeded solution was added, and then reaction mixture was gently mixed for 10 s and left undisturbed for at least 3 hours. Au nanorods were collected with centrifugation (×1000 g, 10 minutes) and redispersion in deionized water in order to remove excessive CTAB surfactant.

Transmission electron microscopy (TEM) of Au nanorods in Figure 1 and hybrid structures in Figure 7 were performed using a JEOL JEM-2100 field-emission TEM system at an acceleration voltage of 200 kV. The hybrid structures are achieved from mixing aqueous solution from each solution of Au nanorods and functionalized SWNTs. The functionalized SWNTs solution was diluted as 0.02 mg/L and the Au nanorod solution also diluted by 1000 times compared to the condensed Au nanorods solution.

Absorption spectra were obtained using a CARY5/CARY 500 UV-Vis-NIR spectrophotometer (Varian Analytical Instrument, CA, USA) from 400 nm to 1200 nm. In the first set of experiments, data were collected 10 minutes after adding 0.02 g/L functionalized SWNTs solution into 3 mL Au nanorods solution. The SWNT solution volumes added were increased from 0 to 25 μL in steps of 10 μL followed by steps of 20 μL from 30 μL to 250 μL. Next, absorption spectra were collected from 0 to 50 μL in steps of 10 μL, each spectrum obtained 1 hour after mixing Au nanorods and functionalized SWNTs in aqueous solution. The final set of experiments were conducted on a fixed mixture of Au nanorods solution with 50 μL of the functionalized SWNT solution in which the time evolution of this mixture was studied by collecting absorption spectra from 1 hour to 11 hours.

3. Results and Discussions

The lengths and widths of Au nanorods are found to be 54 ± 11 nm and 13 ± 3 nm, respectively, using TEM images. Thus, the average aspect ratio of Au nanorods is approximately 4.2 ± 1 (Figure 1(a)). It is well established in the literature that the absorption spectrum of Au nanorods is determined by their size and shape distribution [11]. The UV-Vis-IR spectrum (Figure 1(b)) exhibits two plasmon

peaks, one at 520 nm due to the transverse surface plasmon mode and another at 765 nm due to the longitudinal surface plasmon mode [19].

The insolubility of carbon nanotubes (CNTs) in most common solvents has been an issue regarding their applications [20]. This adverse situation must be overcome to achieve hybrid composite structures in aqueous solutions. In the present work, we used chemical functionalization with polymer (PSS) to optimize applications of SWNTs [16]. Figure 2 shows that the functionalized SWNTs used are uniformly distributed in water.

Figure 3(a) shows absorption spectra of Au nanorod solutions with varying amounts of functionalized SWNTs. Here, each spectrum was collected 10 minutes after the corresponding sample concentration was developed. A Lorentzian function was used to peak fit the longitudinal plasmon mode for each new sample mixture. The resulting absorption profiles indicate a lower energy shift in the peak position along with a decrease in the peak intensity of the longitudinal modes as the functionalized SWNTs concentrations are increased, whereas the transverse mode at 520 nm is unaltered. In addition, a new peak appears between 1000 and 1100 nm for the higher concentrations of SWNT-PSS^{n-}. Figure 3(b) shows the peak positions of both the transverse and longitudinal plasmon modes as the concentration of the functionalized SWNTs is increased. The absorption intensities of both surface plasmon resonances (SPRs) are directly related to the number of Au nanorods in the aqueous solution. Once again, changes are observed only in the profile of the longitudinal plasmon peak. Since the number of Au nanorods remains unaltered in these measurements, this indicates possible changes in the arrangement of the Au nanorods.

Figure 4 shows absorption spectra obtained from these mixed Au nanorod/functionalized SWNT solutions over a lower concentration range of the SWNT-PSS^{n-}. However, each new mixed solution is studied after a one-hour time interval following its preparation. Figure 4(a) shows that increasing the SWNT-PSS^{n-} concentrations in these mixed solutions results in a similar red shifting of the longitudinal plasmon peak along with a decrease in the peak intensity and a broadening in the peak width. Once again, new structure appears between 1000 and 1100 nm in the absorption spectra which increases in intensity as more functionalized SWNTs are added to the mixture. Figure 4(b) shows the red-shift in absorption peak of the longitudinal plasmon mode while, once again, no peak position changes appear in the transverse plasmon mode. The slope of the longitudinal plasmon peak positions in Figure 4(b) is larger than the slope of Figure 3(b), even though concentrations of functionalized SWNTs in Figure 4(a) are lower than those appearing in Figure 3(a). It is clearly seen from these absorption spectra that there are significant structural arrangements occurring when the time following sample preparation is increased from 10 minutes (Figure 3) to one hour (Figure 4).

The effect of the time evolution following preparation on the absorption spectra is illustrated in Figure 5. Here the amount of functionalized SWNT is maintained after 50 μL of 0.02 g/L SWNT-PSS^{n-} was added to the Au nanorod solution. Interactions of the Au nanorods and functionalized SWNTs in aqueous solution appear significant within the first 2 hours following sample preparation. However, no noticeable changes in absorption are observed after this 2-hour time interval. Overall, within 2 hours of sample preparation, the peak position of the longitudinal mode is not shifted while the absorption intensity of this mode decreases. In addition, a significant structure appears between 1000 and 1100 nm.

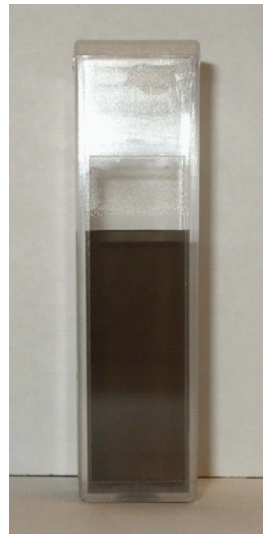

Figure 2: 0.02 g/L of functionalized SWNTs (SWNT-PSS^{n-}) in a cuvette. The functionalized SWNTs appear well suspended in the DI water.

Similar trends are observed in Figures 3, 4, and 5 with the change of concentration of functionalized SWNTs in the Au nanorod solutions. The longitudinal surface plasmon peak is observed to shift via concentration changes of functionalized SWNTs, but the transverse peak is not affected. The spectral behaviors observed in Figures 3 and 4 indicate that linear changes occur in the peak position of the longitudinal surface plasmon with concentration changes of functionalized SWNTs. Also, new structure appears between 1000 and 1100 nm. The fact that the transverse plasmon modes are not changing in their appearance, but that the longitudinal peaks undergo both a gradual decrease in their intensity and a red shift in their position, indicates a new hybrid composition between the Au nanorods and the functionalized SWNTs. Since the longitudinal plasmon mode is related to the long axis of the nanorods [19, 21–23], this suggests a possible end-to-end arrangement of the gold nanorods utilizing the functionalized SWNTs as a template. Hence, we attribute the 1000–1100 nm band to hybridization of the longitudinal plasmon modes due to strong electromagnetic coupling [24, 25]. The systematic decrease in the intensity of regular longitudinal mode (i.e., 765 nm) with increasing SWNT concentration or time is owed to the creation of end-to-end-coupled nanorod structures at the expense of isolated (singular) ones, as also argued by Park et al. for their end-to-end assembly of Au nanorods by lyotropic chromonic

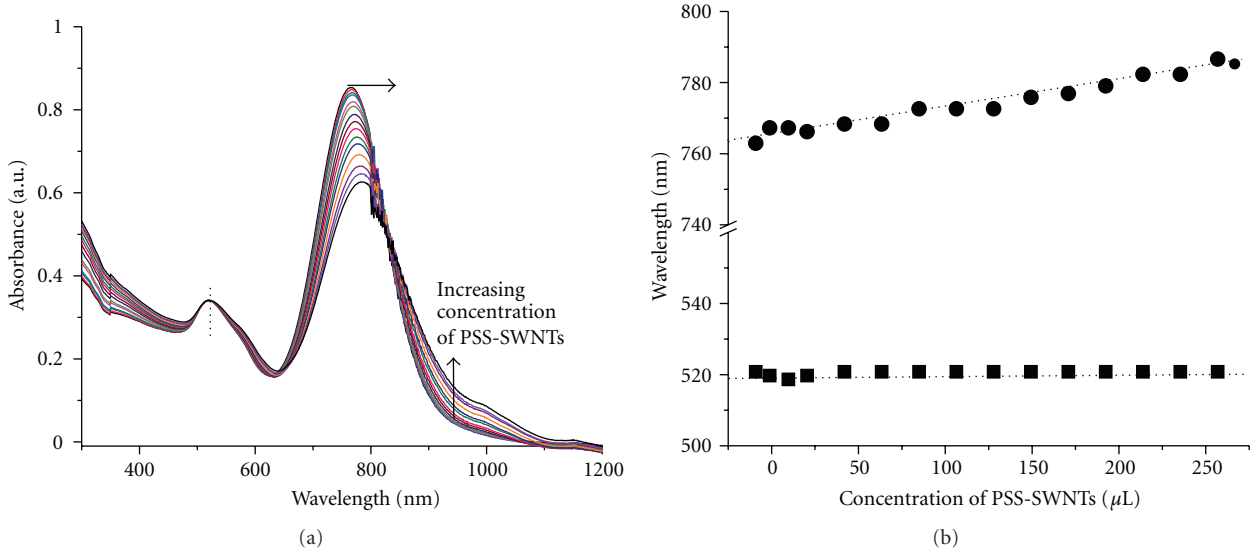

Figure 3: (a) UV-Vis-IR spectra of gold nanorod suspensions for varying concentration of functionalized SWNTs. Each spectrum was collected 10 minutes after sample preparation. (b) Corresponding peak wavelength of the longitudinal and transverse plasmon modes of the Au nanorods.

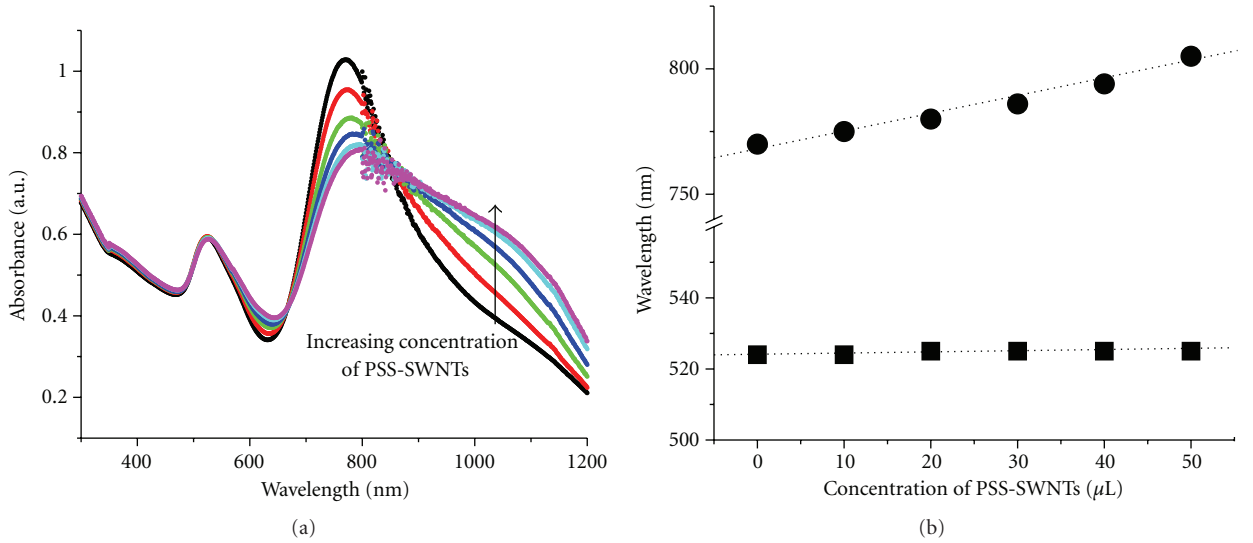

Figure 4: (a) UV-Vis-IR spectra of gold nanorods for varying concentration of functionalized SWNTs. Each spectrum was collected 60 minutes after adding PSS-SWNTs. (b) Corresponding peak wavelength of the longitudinal plasmon mode and transverse plasmon mode of the Au nanorods.

materials [24]. The basis for the self-arrangement in our work is that the SWNTs functionalized by PSS have high densities of negatively charged sulfonate groups, whereas Au nanorods, capped by cetyltrimethylammonium bromide (CTAB), are positively charged. As a result, the Au nanorods are attracted to the surfaces of SWNT-PSS^{n-} [21–23]. The process of self-assembly of Au nanorods on the surface of a functionalized SWNT is schematically illustrated in Figure 6. The gradual lower energy shift of the regular longitudinal plasmon mode in Figures 3–5 is credited to electromagnetic coupling between the single nanorods and the SWNT substrates after attachment [21, 23]. This interpretation is supported by the research of Correa-Duarte et al. [21] who indicated that multiwalled carbon nanotubes act as templates for three different aspect ratios of Au nanorods for fabricating hybrid structures. The experimental measurements of the UV-Vis-IR spectroscopy support this idea as shown in Figure 6.

The TEM images shown in Figure 7 also support self-assembly of the Au nanorods on the surface of functionalized SWNTs. The four TEM images are acquired from hybrid structures of gold nanorods and functionalized SWNTs in various magnifications. The TEM samples were prepared by combining a solution of functionalized SWNTs with a

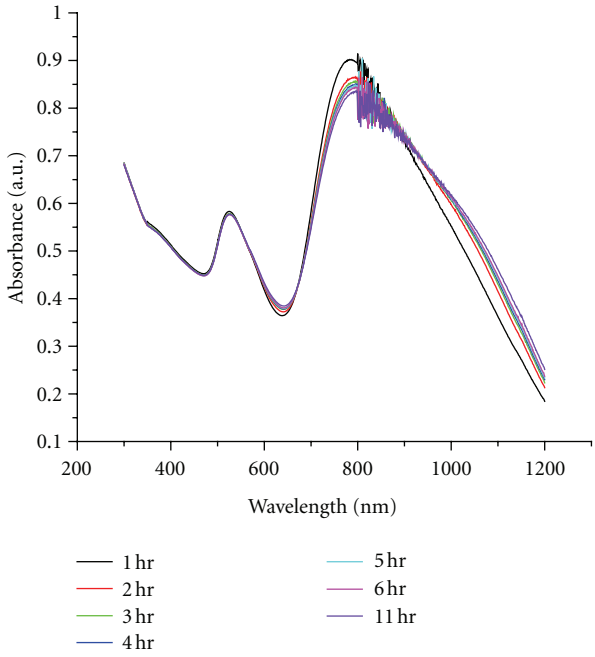

Figure 5: Time evolution of the UV-Vis-IR absorption spectrum of the Au nanorods in deionized water (3 mL) after 50 μL of 0.02 g/L SWNT-PSS^{n-} is added. After two hours, no further significant changes appear in the absorption spectrum.

solution of Au nanorods for 20 minutes of mixing. The red solid arrows in these images indicate functionalized SWNTs in the prepared samples. The extensive aggregation of gold nanorods most probably results from the drying process on the TEM grid. Such aggregation is unlikely to have occurred in the solution that would have otherwise led to a change in the transverse surface plasmon resonance peak at 520 nm. Despite this undesirable aggregation in TEM imaging, the self-assembly of gold nanorods along the surfaces of functionalized SWNTs is clearly distinguishable as seen in Figure 7(a). Further verification of the alignment of the gold nanorods along the surfaces of functionalized SWNTs is shown in Figures 7(b)–7(d).

Further evidence of this structural arrangement is the appearance of an isosbestic point at approximately 860 nm in Figure 4(a) that results from the gradual decrease of the intensity of the longitudinal mode along with the simultaneous appearance of new structure between 1000 and 1100 nm. In general, the maximum intensities of localized plasmon resonances are very sensitive to the aspect ratios of pure gold nanorods [26]. In our case, the appearance of the isosbestic point in the measured absorption spectra results from the interaction between the Au nanorods with the increasing concentration changes of the functionalized SWNTs [27]. The end-to-end alignment between adjacent Au nanorods assembling on the surface of a carbon nanotube results in hybrid structure of Au nanorods and functionalized SWNT, which is consistent with the appearance of the new absorption structure between 1000 and 1100 nm (Figures 3–5) and the illustration in Figure 6 [24, 25, 28].

The new absorption structure between 1000 and 1100 nm of these hybrid composites could also be explained by the emergence of an absorption peak associated with semiconducting SWNTs. However, the largest concentration of functionalized SWNTs used in our study is considerably lower as compared to that of the gold nanorods in these aqueous solutions (1/61). Thus, we feel that electronic transitions in SWNTs are not the cause of the new structure observed in Figures 3 to 5.

The gradual redshift of the longitudinal plasmon peak at 765 nm (Figures 4 and 5) is also attributed to nanorod-nanorod coupling, which is, however, at a weaker level than that for nanorods in the end-to-end arrangement. In other words, strong plasmon coupling in the end-to-end-arranged rod population yields the hybrid plasmon mode peaking at 1000–1100 nm [29]. On the other hand, coupling of the longitudinal modes between nanorods of larger separation is thought to be responsible for the gradual shift of the 765 nm peak. The plasmonic properties of metallic nanoparticles are strongly dependent on interparticle interactions [30]. Since a gold nanorod can interact with an adjacent nanorod in close proximity on the surface of functionalized SWNT, the spectral shift of longitudinal or transverse plasmon maxima is dependent on the population fraction of assemblies or arrays of hybrid gold nanorods [25, 31–33].

Increasing the number of gold nanorods assembled on the surface of a SWNT reduces the gap between adjacent nanorods along the long-axis direction. Recently, Gunnarsson et al. [34] have observed plasmon frequency shifts with varying interparticle gaps using Ag nanodisc pairs. The interparticle model is not perfectly matched with this system, but it helps in understanding the redshifts observed in the longitudinal plasmon mode. Interestingly, the transverse plasmon mode does not show any spectral shift, which indicates no coupling between gold nanorods along the vertical (radial) direction. Therefore, the nanorods are inferred to align end to end and not side by side. The small broadening observed in the transverse plasmon mode could be due to a limited interaction with the radial volume of the SWNT. The spectral behavior of transverse plasmon mode also supports the alignment of gold nanorods on surface of functionalized SWNTs.

4. Conclusion

We have demonstrated a simple methodology to fabricate nanohybrid composites in aqueous solutions. We have observed changes in the absorption spectra of these composites as a result of the self-assembly, driven by the electrolyte interaction of the Au nanorod and the SWNT-PSS^{n-}. The TEM images support the self-assembly of gold nanorods on surfaces of functionalized SWNTs. The dependency of the absorption spectra on the concentration of the functionalized SWNTs suggests that it is possible to manipulate the optical properties through the formation of these hybrid nanocomposite structures. We believe these attributes could be exploited in fabrication of nanohybrid devices.

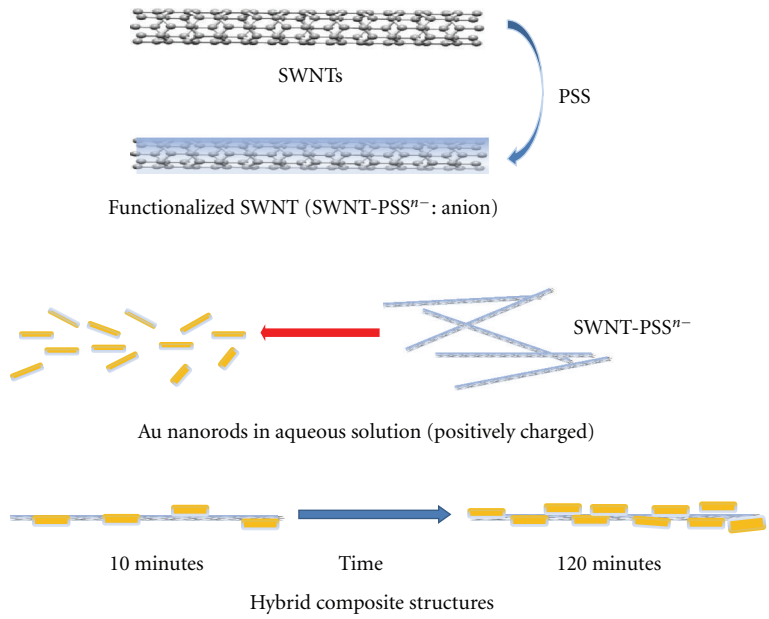

Figure 6: Schematic illustration of the main processes taking place during the formation and arrangement of Au nanorods and functionalized single-walled carbon nanotubes.

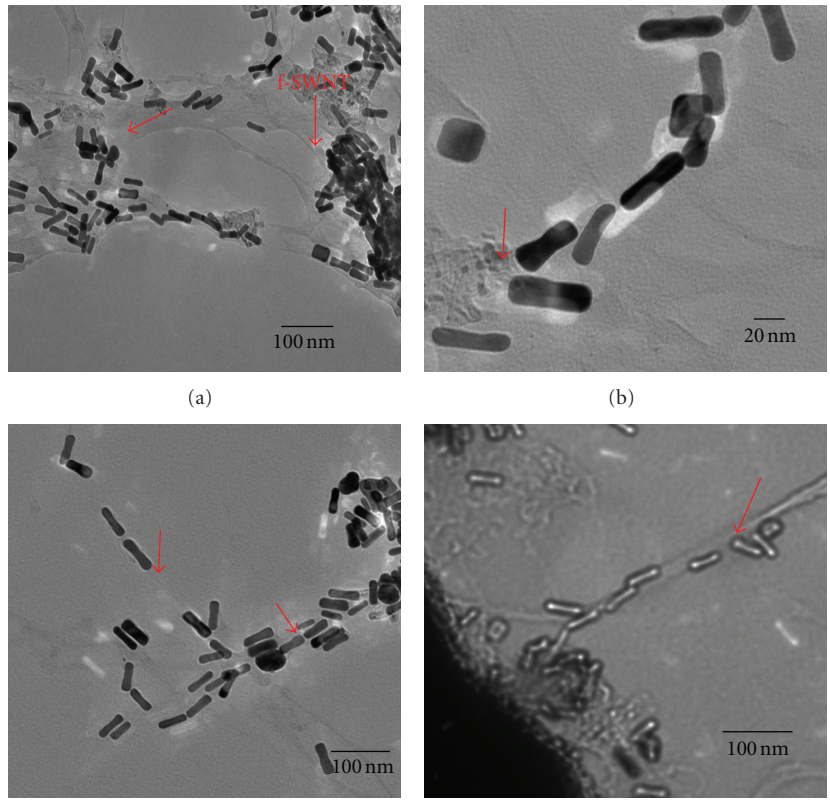

Figure 7: TEM images of hybrid structures of gold nanorods and functionalized SWNTs in various magnifications (a)–(d). (Red solid arrows in images indicate functionalized SWNTs). The mixed solution was dried out for less than 20 minutes for TEM. The functionalized SWNTs solution was diluted as 0.02 mg/L, and Au nanorods solution also diluted by 1000 times compared to the condensed Au nanorods solution.

Acknowledgments

The authors thank H. James Harmon for allowing the use of his laboratory and the CARY5/CARY 500 UV-Vis-NIR spectrophotometer. They also thank Warren T. Ford for fruitful discussions. This work has been supported, in part, by the NSF EPSCoR award EPS 0814361, by the NSF award ECCS-0601362, and by the Oklahoma Center for the Advancement of Science and Technology award AR072-066.

References

[1] Y. Zhang, T. F. Kang, Y. W. Wan, and S. Y. Chen, "Gold nanoparticles-carbon nanotubes modified sensor for electrochemical determination of organophosphate pesticides," *Microchimica Acta*, vol. 165, no. 3-4, pp. 307–311, 2009.

[2] P. L. Ong, W. B. Euler, and I. A. Levitsky, "Hybrid solar cells based on single-walled carbon nanotubes/Si heterojunctions," *Nanotechnology*, vol. 21, no. 10, Article ID 105203, 2010.

[3] P. Gao, H. Li, Q. Zhang, N. Peng, and D. He, "Carbon nanotube field-effect transistors functionalized with self-assembly gold nanocrystals," *Nanotechnology*, vol. 21, no. 9, Article ID 095202, 2010.

[4] A. Gole and C. J. Murphy, "Azide-derivatized gold nanorods: functional materials for "click" chemistry," *Langmuir*, vol. 24, no. 1, pp. 266–272, 2008.

[5] M. Salsamendi, J. Abad, R. Marcilla et al., "Synthesis and electro-optical characterization of new conducting PEDOT/Au-nanorods nanocomposites," *Polymers for Advanced Technologies*, vol. 22, no. 12, pp. 1665–1672, 2011.

[6] M. Salsamendi, R. Marcilla, M. Döbbelin et al., "Simultaneous synthesis of gold nanoparticles and conducting poly(3,4-ethylenedioxythiophene) towards optoelectronic nanocomposites," *Physica Status Solidi (A) Applications and Materials*, vol. 205, no. 6, pp. 1451–1454, 2008.

[7] C. Yu and J. Irudayaraj, "Multiplex biosensor using gold nanorods," *Analytical Chemistry*, vol. 79, no. 2, pp. 572–579, 2007.

[8] X. Ren, D. Chen, X. Meng, F. Tang, A. Du, and L. Zhang, "Amperometric glucose biosensor based on a gold nanorods/cellulose acetate composite film as immobilization matrix," *Colloids and Surfaces B*, vol. 72, no. 2, pp. 188–192, 2009.

[9] G. M. A. Rahman, D. M. Guldi, E. Zambon, L. Pasquato, N. Tagmatarchis, and M. Prato, "Dispensable carbon nanotube/gold nanohybrids: evidence for strong electronic interactions," *Small*, vol. 1, no. 5, pp. 527–530, 2005.

[10] M. Abdulla-Al-Mamun, Y. Kusumoto, A. Mihata, M. S. Islam, and B. Ahmmad, "Plasmon-induced photothermal cell-killing effect of gold colloidal nanoparticles on epithelial carcinoma cells," *Photochemical and Photobiological Sciences*, vol. 8, no. 8, pp. 1125–1129, 2009.

[11] K. L. Kelly, E. Coronado, L. L. Zhao, and G. C. Schatz, "The optical properties of metal nanoparticles: the influence of size, shape, and dielectric environment," *Journal of Physical Chemistry B*, vol. 107, no. 3, pp. 668–677, 2003.

[12] A. Gole and C. J. Murphy, "Seed-mediated synthesis of gold nanorods: role of the size and nature of the seed," *Chemistry of Materials*, vol. 16, no. 19, pp. 3633–3640, 2004.

[13] C. A. Dyke and J. M. Tour, "Solvent-free functionalization of carbon nanotubes," *Journal of the American Chemical Society*, vol. 125, no. 5, pp. 1156–1157, 2003.

[14] V. A. Sinani, M. K. Gheith, A. A. Yaroslavov et al., "Aqueous dispersions of single-wall and multiwall carbon nanotubes with designed amphiphilic polycations," *Journal of the American Chemical Society*, vol. 127, no. 10, pp. 3463–3472, 2005.

[15] T. K. Sau and C. J. Murphy, "Seeded high yield synthesis of short Au nanorods in aqueous solution," *Langmuir*, vol. 20, no. 15, pp. 6414–6420, 2004.

[16] S. Qin, D. Qin, W. T. Ford et al., "Solubilization and purification of single-wall carbon nanotubes in water by in situ radical polymerization of sodium 4-styrenesulfonate," *Macromolecules*, vol. 37, no. 11, pp. 3965–3967, 2004.

[17] N. R. Jana, L. Gearheart, and C. J. Murphy, "Wet chemical synthesis of high aspect ratio cylindrical gold nanorods," *Journal of Physical Chemistry B*, vol. 105, no. 19, pp. 4065–4067, 2001.

[18] C. J. Murphy and N. R. Jana, "Controlling the aspect ratio of inorganic nanorods and nanowires," *Advanced Materials*, vol. 14, no. 1, pp. 80–82, 2002.

[19] J. Pérez-Juste, I. Pastoriza-Santos, L. M. Liz-Marzán, and P. Mulvaney, "Gold nanorods: synthesis, characterization and applications," *Coordination Chemistry Reviews*, vol. 249, no. 17-18, pp. 1870–1901, 2005.

[20] C. A. Dyke and J. M. Tour, "Overcoming the insolubility of carbon nanotubes through high degrees of sidewall functionalization," *Chemistry—A European Journal*, vol. 10, no. 4, pp. 812–817, 2004.

[21] M. A. Correa-Duarte, J. Pérez-Juste, A. Sánchez-Iglesias, M. Giersig, and L. M. Liz-Marzán, "Aligning Au nanorods by using carbon nanotubes as templates," *Angewandte Chemie—International Edition*, vol. 44, no. 28, pp. 4375–4378, 2005.

[22] K. G. Thomas, S. Barazzouk, B. I. Ipe, S. T. S. Joseph, and P. V. Kamat, "Uniaxial plasmon coupling through longitudinal self-assembly of gold nanorods," *Journal of Physical Chemistry B*, vol. 108, no. 35, pp. 13066–13068, 2004.

[23] M. A. Correa-Duarte and L. M. Liz-Marzán, "Carbon nanotubes as templates for one-dimensional nanoparticle assemblies," *Journal of Materials Chemistry*, vol. 16, no. 1, pp. 22–25, 2006.

[24] H. S. Park, A. Agarwal, N. A. Kotov, and O. D. Lavrentovich, "Controllable side-by-side and end-to-end assembly of Au nanorods by lyotropic chromonic materials," *Langmuir*, vol. 24, no. 24, pp. 13833–13837, 2008.

[25] P. K. Jain, S. Eustis, and M. A. El-Sayed, "Plasmon coupling in nanorod assemblies: optical absorption, discrete dipole approximation simulation, and exciton-coupling model," *Journal of Physical Chemistry B*, vol. 110, no. 37, pp. 18243–18253, 2006.

[26] S. Link, M. B. Mohamed, and M. A. El-Sayed, "Simulation of the optical absorption spectra of gold nanorods as a function of their aspect ratio and the effect of the medium dielectric constant," *Journal of Physical Chemistry B*, vol. 103, no. 16, pp. 3073–3077, 1999.

[27] D. M. Guldi, G. M. A. Rahman, F. Zerbetto, and M. Prato, "Carbon nanotubes in electron donor—acceptor nanocomposites," *Accounts of Chemical Research*, vol. 38, no. 11, pp. 871–878, 2005.

[28] J. T. Lin, Y. L. Hong, and C. L. Chang, "A nonlinear optical theory of gold nanorods," in *Nanoscale Imaging, Sensing, and Actuation for Biomedical Applications VII*, vol. 7574 of *Proceedings of SPIE*, 2010.

[29] G. Lu, O. K. Farha, L. E. Kreno et al., "Fabrication of metal-organic framework-containing silica-colloidal crystals for vapor sensing," *Advanced Materials*, vol. 23, no. 38, pp. 4449–4452, 2011.

[30] B. Lamprecht, G. Schider, R. T. Lechner et al., "Metal nanoparticle gratings: influence of dipolar particle interaction on the plasmon resonance," *Physical Review Letters*, vol. 84, no. 20, pp. 4721–4724, 2000.

[31] P. K. Jain, W. Huang, and M. A. El-Sayed, "On the universal scaling behavior of the distance decay of plasmon coupling in metal nanoparticle pairs: a plasmon ruler equation," *Nano Letters*, vol. 7, no. 7, pp. 2080–2088, 2007.

[32] K. H. Su, Q. H. Wei, X. Zhang, J. J. Mock, D. R. Smith, and S. Schultz, "Interparticle coupling effects on plasmon resonances of nanogold particles," *Nano Letters*, vol. 3, no. 8, pp. 1087–1090, 2003.

[33] W. Rechberger, A. Hohenau, A. Leitner, J. R. Krenn, B. Lamprecht, and F. R. Aussenegg, "Optical properties of two interacting gold nanoparticles," *Optics Communications*, vol. 220, no. 1-3, pp. 137–141, 2003.

[34] L. Gunnarsson, T. Rindzevicius, J. Prikulis et al., "Confined plasmons in nanofabricated single silver particle pairs: experimental observations of strong interparticle interactions," *Journal of Physical Chemistry B*, vol. 109, no. 3, pp. 1079–1087, 2005.